Int. J. Electrochem. Sci., 16 **(2021)** Article Number: 211113, doi: 10.20964/2021.11.32

International Journal of
ELECTROCHEMICAL
SCIENCE
www.electrochemsci.org

Ab Initio Studies of Li_3AlH_6 Materials for Hydrogen Storage Purposes and Optoelectronic Applications

Madiha Makhdoom[1], Sikander Azam[2,], Abdul Waheed[3], Ambreen Kalsoom[4,*], Azhar Iqbal[1], Bakhtiar Ul Haq[5], S. S. Ahmad[6], Imran Zada[6], Sarzamin Khan[7]*

[1] Department of Physics, School of Science, University of Management and Technology Lahore, Pakistan
[2] Faculty of Engineering and Applied Sciences, Department of Physics, RIPHAH International University I-14 Campus Islamabad, Pakistan
[3] Department of Geotechnical Engineering MCE, NUST Risalpur, Pakistan
[4] Department of Physics, The Government Sadiq College Women University, Bahawalpur, Pakistan
[5]Advanced Functional Materials & Optoelectronics Laboratory (AFMOL), Department of Physics, Faculty of Science, King Khalid University, P.O. Box 9004, Abha, Saudi Arabia
[6] Department of Physics, University of Swabi, Pakistan
[7] Department of Chemistry, University of Swabi, Pakistan
[*]E-mail: sikander.physicst@gmail.com, Kalsoom.ambreen@gscwu.edu.pk

Received: 6 July 2021 / *Accepted:* 31 August 2021 / *Published:* 10 October 2021

Hydrogen storage is a definitive step for commercialization of energy production. The solid stated method of hydrogen storge gained much attention in current research, instead of large number of storage thehniques. This research rationally shows the optoelectronic properties of Li_3AlH_6 using computational method. The structrual, density of states and corresponding optical and electrical properties of Li_3AlH_6 was investigated. Firstly, we optimize the crystal structures of solid state Li_3AlH_6 hydrides. Furthermore, electronic and optical band structures of hydrides is computed. The Li_3AlH_6 have indirect bands gap as 2.97 eV (N-Γ). Thus, the investigating material is electronically semiconducting. This indicates that Li_3AlH_6 has a deep influence on its electronic structure and optical properties, which is the goal of theoretical basis for research to be achieved.

Keywords: Hydrogen storage material, Optoelectronic properties, FP-LAPW, DFT.

1. INTRODUCTION

The primary requirement for the effective use of hydrogen energy is storage of the hydrogen gas at appropriately high energy density in order to make it practically useful and effective. There are various methods used for the storage of hydrogen. One method is to store high pressure gaseous

hydrogen in cylindrical containers. Another method is to store liquid hydrogen at atmospheric pressure and very low temperature of about 20 K in cryogenic tanks [1]. But the aforementioned methods are practically not feasible because of the problems of safety, economics and limitations on volume of hydrogen being stored [4]. For example, the hydrogen as a high pressure compressed gas has very heavy containers of huge volumes which in turn become too risky to be used in automobiles. On the other hand, storage of hydrogen in liquid state requires huge amount of energy and thus it becomes highly uneconomical. So, the most effective, safer and practically achievable method used for the storage of hydrogen is to store hydrogen in solid substances. Hydrides of metals [5, 6], impregnated activated charcoals [7, 8] and some compounds of carbon like nanotubes and nanofibers of carbon and activated carbon [9, 10, 11] have been found to have hydrogen storage property. The solid state material used in hydrogen storage must be able to fulfill certain requirements in order to be used for the said purpose. First of all, the material should be able to perform consistently with regard to hydrogen storage capacity and kinetics after cycling as well [12] so that it can repeatedly release and absorb hydrogen (by regulating pressure and/or temperature) and does not damage the storage material [13]. Secondly, its stability should not be very high so that release of hydrogen is possible without too much heating and its hydrogen/metal ratio must be high enough, so the investigation of stability of the meal hydrides is of vital importance in order to design practically useful hydrogen storage materials [14]. Thirdly, the material should be able to react reversibly with hydrogen during repeated absorption and desorption [13].

Hydrides of metals and complex hydrides are materials of great interest because they have very high content of hydrogen, good absorption and desorption kinetics of hydrogen operating systems of temperature and pressure, good volumetric and gravimetric capacities and low weight. So, metal and complex hydrides have thoroughly been studied theoretically as well as experimentally as hydrogen storage substances [3]. Hydrogen is stored in metal hydrides by an intermetallic alloy phase in which chemical bonds absorb and store hydrogen [15].

Up to our understanding, we found no comprehensive work in literature using the ab -initio calculations on the electronic and optical properties of Li_3AlH_6 compound. Due this reason we have performed a detailed calculations of the electronic, and optical properties of Li_3AlH_6 compound by using full-potential method. The GGA approximation has been used for the exchange- correlation potential as a result that the f electrons can be accurately treated. Our calculations will demonstrate the effect of using a full-potential method on the electronic and optical properties of Li_3AlH_6 compound.

Next section presents the calculation methods. Section 3 discusses the results of structural properties, electronic band structure, total and partial density of states, electronic charge density and optical properties. The conclusion of our result is given in the last section.

2. METHODOLOGY

2.1. Theoretical framework

Here in we studied theoretically the electronic and optical properties of the Li_3AlH_6 by using full potential linear augmented plane wave (FPLAPW) method. The material Li_3AlH_6 has the

monoclinic symmetry. We take the crystallographic data from the material project. It's space group is trigonal [Space group $R\bar{3}$[148]] phase, see crystal structure in Fig. 1.

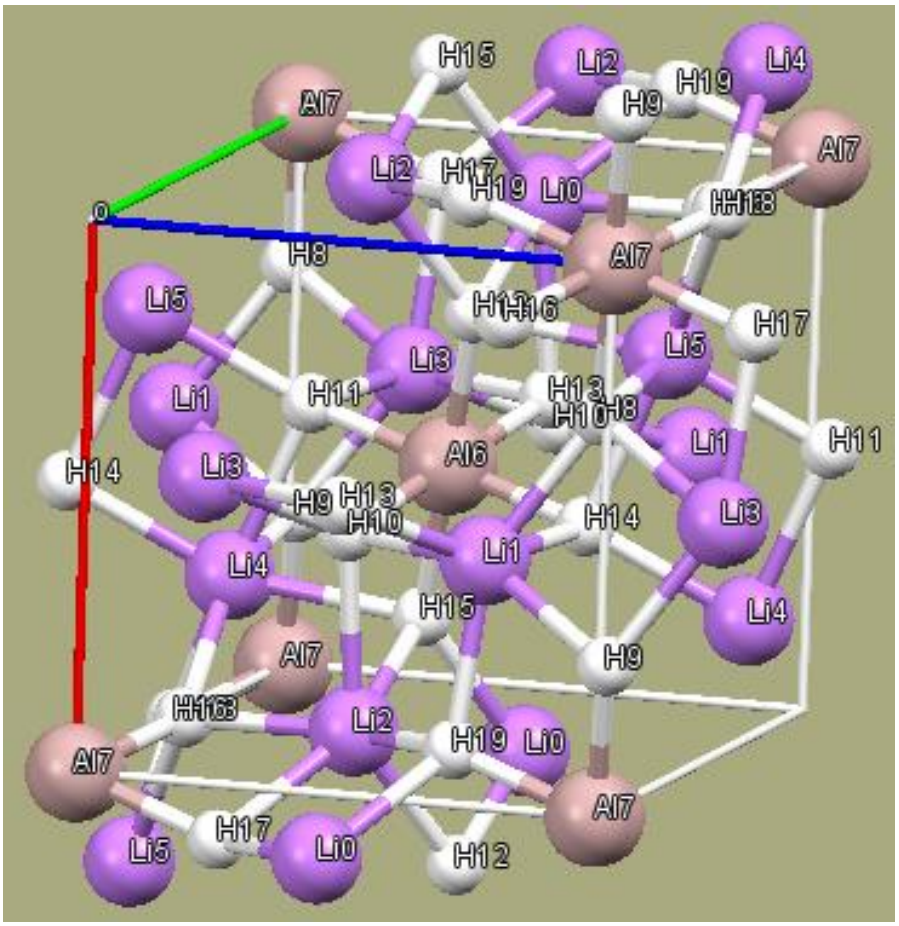

Figure 1. Unit cell structure of Li_3AlH_6

2.2. Calculation method

We performed our calculations by full-potential method (FPLAPW) endorsed in the WIEN2k programs [16]. The generalized gradient approximation (GGA) exchange–correlation potential were used to treat the exchange correlation [17-19]. The sphere radii used for Li, Al and H is 2.00 a.u. We achieved converged solutions with $R_{MT}\times K_{max}=7.0$, R_{MT} is the muffin-tin radii, while K_{max} is the plane wave cut-off. Brillouin zone (BZ) integrations in the self-consistency cycles were executed by means of tetrahedron symmetry [20], 2000 k-points in the irreducible BZ is used.

2.3. Theoretical description of optical properties

In solid materials the optical reaction is often expressed by the complex dielectric function $\varepsilon(\omega)=\varepsilon_1(\omega)+i\varepsilon_2(\omega)$. According to the definitions of direct transition probabilities and Kramers–Kronig dispersion relations, the real and imaginary parts parts of the dielectric function,

absorption coefficient, reflectivity and complex optical conductivity is computed by considering the following theoretical formula:

$$\varepsilon_2(\omega) - = \frac{\pi e^2}{\varepsilon_0 m^2 \omega^2} \sum_{V,C} \{ \int_{BZ} \frac{2dk}{(2\pi)^2} \left| a \times M_{V,C} \right|^2 \delta[E_C(k) - E_V(k) - \hbar\omega] \} \ldots\ldots. (3)$$

$$\varepsilon_1(\omega) = 1 + \frac{2e}{\varepsilon_0 m^2} \times \varepsilon_{V,C} \int_{BZ} \frac{2dk}{(2\pi)^2} \frac{\left| a \times M_{V,C}(k) \right|^2}{E_C(k) - E_V(k)/\hbar} \times \frac{1}{[E_C(k) - E_V(k)]^2/\hbar^2 - \omega^2} \ldots (4)$$

Starting from dielectric function $(\varepsilon(\omega))$, the other realated optical parameters like reflectivity $(R(\omega))$, absorption $(I(\omega))$, refractivity $(n(\omega))$, extinction co-efficient $(k(\omega))$ and energy loss function $(L(\omega))$ can then be calculated

$$\alpha(\omega) = \frac{2k\omega}{c} = \frac{2\pi k}{\lambda_0} \ldots.. (5)$$

$$R(\omega) = \left| \frac{\sqrt{\varepsilon_1(\omega) + j\varepsilon_2(\omega)} - 1}{\sqrt{\varepsilon_1(\omega) + j\varepsilon_2(\omega)} + 1} \right| \ldots\ldots (6)$$

$$L(\omega) = \varepsilon_2(\omega) / [\varepsilon_1^2(\omega) + \varepsilon_2^2(\omega)]$$

$$n(\omega) = \frac{1}{\sqrt{2}} \left[\sqrt{\varepsilon_1^2(\omega) + \varepsilon_2^2(\omega)} + \varepsilon_1(\omega) \right]^{1/2}$$

The terms n, k, ε_0, λ_0, C, V, BZ, and K, represents the refractive index, extinction coefficient, dielectric constant, wavelength of light in vacuum, conduction band, valence band, the first Brillouin zone and electron wave vector, respectively.

2.4. Electronic structure

This portion of the manuscript shows the result on the optoelectronic properties like band structures (BS), densities of states (DOS) and optical spectra of the mentioned material. The band structures along with total and partial density of states (TDOS and PDOS) are plotted in Figs. 3 and 4, respectively. The investigated optimized crystal structure along the high symmetry directions G→H→N→G→P for Li_3AlH_6 is portrayed in Fig. 2. It is noticeable from the band structure spectra that the bands are less dispersive, this small dispersion of bands insinuate that electrons and hole effective mass is smaller but in reflection their mobility is greater. The band structure shows indirect band gap of 2.971 eV, the highest energy of valence bands is located at N point and conduction bands at located at G point.

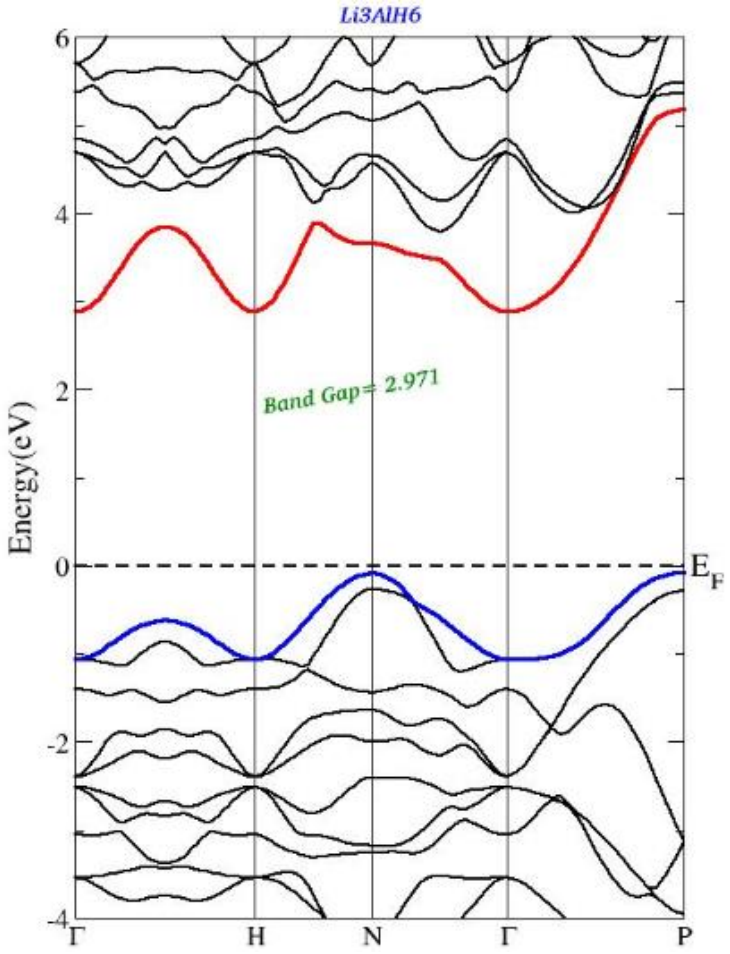

Figure 2. Calculated band structure of Li_3AlH_6

To understand the nature of electronic distributions, we calculated the total and partial densities of states (DOS) that describe electron distribution in an energy spectrum for Li_3AlH_6 compound as presented Fig. 4. The Fig. 3 shows the electronic states in the computed compound are separated into three regions including valence band (in two regions) and conduction band (in one region) by a gap. The valence band states have a breadth of about 8.0 eV.

As shown in Figs. 4, which the lowest energy bands of the VB, in the energy range -8.0 to -6.0 eV comes from Al-s state with some contribution H/Li-s states. The bands, at energy range from -6.0 to 0.0 eV that comes from Al-p and H-s states with minor contribution from Li/Al-s states. The conduction band from 3.0 to 6.0 eV is mainly comprised of Al-s state along with the minor contribution from other states. The top most part of the conduction band is mainly comprised from Al-p state along with the small role of the other states.

The CB is well dispersed and consists of the contribution of Al-s orbital. There exist hybridization between s and p state of Al along with H-s and Li-s state. This hybridization will reflect the strong covalent bonding between these states.

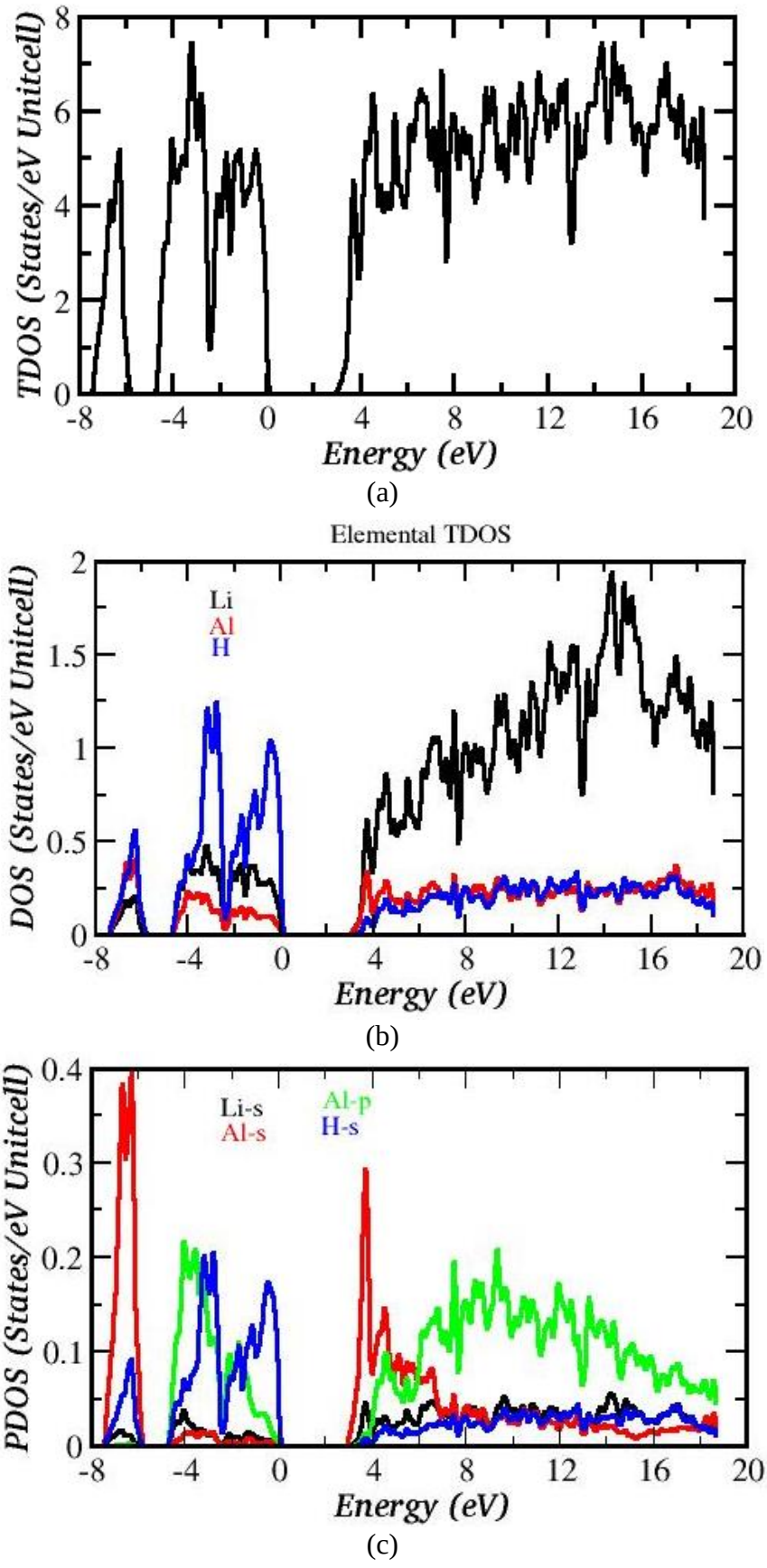

Figure 3. Calculated total and partial densities of states (States/eV unit cell) of Li_3AlH_6

2.5. Linear optical properties

The optical properties, are carried out in the random phase approximation (RPA). The dielectric function $(\varepsilon(\omega))$ is considered very important factor in order to evaluate the band structure and transition energy. Studying the optical properties of semiconductor materials is very important for understanding its application in optoelectronic devices. The dielectric function $(\varepsilon(\omega))$ was investigated in order to give the detail about the optical absorption. Here in we discussed the complex dielectric function $(\varepsilon(\omega)=\varepsilon_1(\omega)+i\varepsilon_2(\omega))$ of the investigated compound. The aborption part $(\varepsilon_2(\omega))$ of the dielectric function basically rely on the density of states and momentum matrix elements. The spectra for the imaginary $(\varepsilon_2(\omega))$ and real $(\varepsilon_1(\omega))$ parts of the dielectric function in range between 0.0 ~ 14.0 eV are depicted in Fig. 5.

The computed compound has the trigonal phase, having two main non zero $\left(\varepsilon^{xx}(\omega)=\varepsilon^{yy}(\omega)\right.$ and $\left.\varepsilon^{zz}(\omega)\right)$ components.

The dispersive part of the dielectric function is depicted in Fig. 4. The static dielectric constant $\varepsilon_1(0)$ are considered important factor of dispersive part, $\varepsilon_1(0)$, of dielectric function, possibly correspond to the reflective index measured at a vibrational frequency. The spectra shows that the $\varepsilon_1(\omega)$ is zero at any photon energies and shows the negative values, that reflects that the incident electromagnetic (E.M) waves are entirely reflected and thus the material shows a conductivecharacter.

The real $\varepsilon_1(\omega)$ part of the complex dielectric function has the maximum energy range between 4.0 ~ 6.0 eV, and beyond this energy limit the spectra shows decrease very sharply reaches to its minimum and zero at about 7.02 eV. Possibly, because of the interband transitions from valence bands to conduction bands exceeding the Fermi level (E_F). The $\varepsilon_1(\omega)$, has been computed from the Kramers–Kronig relations (KKR). The static dielectric real function named as zero frequency is mostly impacted by the energy band gap. The calculated static values are 4.0 and 3.6 for $\varepsilon^{xx}(0)=\varepsilon^{yy}(0)$ and $\varepsilon^{zz}(0)$. These values accord with the band gap, larger the energy gap (E_g) reflect a larger $\varepsilon_1(0)$value, that is elucidated from the Penn model [21]. This (Penn) model is based on this formula $\varepsilon(0)=1+(\hbar\omega_p/E_g)^2$. Showing that, that $\varepsilon(0)$ is inversely proportional to E_g.

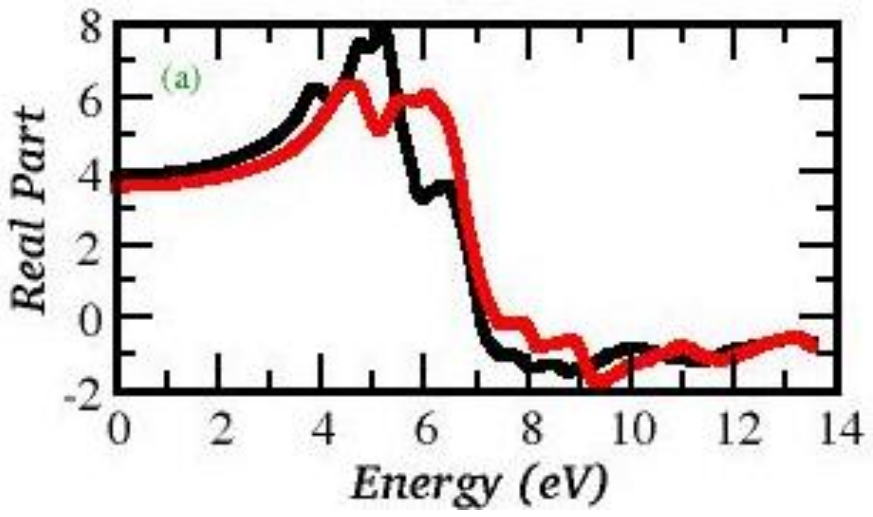

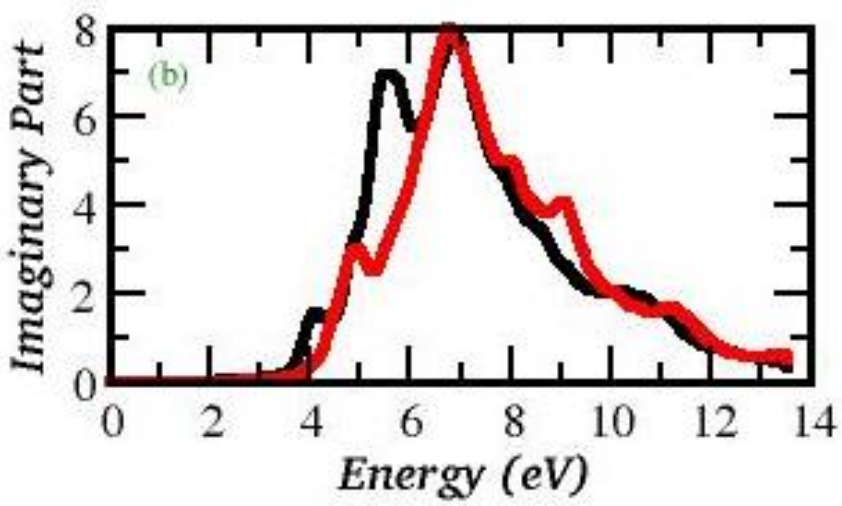

Figure 5. (a) Calculated real part $\varepsilon_1^{xx}(\omega)$ (dark solid curve-black color online) and $\varepsilon_1^{zz}(\omega)$ (red solid curve-black color online) spectra of Li_3AlH_6 **(b)** computed imaginary part $\varepsilon_2^{xx}(\omega)$ (dark solid curve-black color online) and $\varepsilon_2^{zz}(\omega)$ (red solid curve-black color online) of Li_3AlH_6

Fig. 4, shows the imaginary parts, $(\varepsilon_2(\omega))$, of the dielectric function along the x–y plane and parallel to the z-axis of the trigonal [Space group $R\bar{3}$[148]] phase. This determines the optical properties directly and related very closely to the interband optical transition. The $\varepsilon_2(\omega)$ of the dielectric function spectra shows the anisotropic behavior. The peaks in the dielectric function $(\varepsilon(\omega))$ shows the electronic transition between the valance and conduction band. The optical response produce peaks of electric-dipole transitions between the occupied and unoccupied bands. Our result shows that the edge of optical absorption for $\varepsilon_2^{xx}(\omega)$= $\varepsilon_2^{yy}(\omega)$ and $\varepsilon_2^{zz}(\omega)$ are positioned at 3.0 eV, which is accord with the optical transition in the valence band (maximum) at N and conduction band (minimum) at Γ -point $\left(N_V - \Gamma_C\right)$ and are recognized as the elementary absorption edge. The other peaks emerges due to the transitions mostly from H to Li-s states. From our computed band structure we can identifies theses transitions. The $\varepsilon_2(\omega)$ spectra shows the maximum peaks at 5.0 ~ 8.0 eV, beyond this energy the peaks shows decrease. This decrease is due to the increase/decrease in the bandwidth of the unoccupied band.

The other optical parameters like absorption co-efficient $(I(\omega))$, reflectivity $(R(\omega))$, energy loss function $(L(\omega))$, refractive index $(n(\omega))$ and extinction co-efficient $(k(\omega))$. In order to know about the complex dielectric tensor $\varepsilon(\omega)$, then it's easy to compute other optical parameters which is the propagation of the EM waves through the material. The plot for the absorption spectra is demonstrated in Fig. 5 (a). The absorption is started almost at 3.0 eV.

Absorption coefficient $(I(\omega))$ point out the percentage of light intensity reduction at the dispersal through unit distance and the $I(\omega)$ can be calculated as

$$\alpha \equiv \frac{2\omega k}{C} = \frac{4\pi k}{\lambda_0}$$

The λ_0 and C symbolize the wavelength and speed of light in vacuum. Our result for the absorption spectra has been depicted in Fig. 5a. The spectra shows the a rapid increase in the

absorption co-efficient with increasing energy, i.e. a strong absorption is observed in between 3.0 eV to about 14.0 eV. The region between 3.0 ~ 14.0 eV comprises of an assorted peaks, which arises due to different electronic transitions. The absorption region width rely on the material band gap.

The energy loss function $L(\omega)$ is considered very significant factor in explaining the loss energy of fast electrons traversing in a substance. The major peaks in $L(\omega)$ signifies that the properties related to plasma resonance (a combined valence electrons oscillation) and the corresponding frequency is the so-called plasma frequency ω_p. The peaks of $L(\omega)$ ($L^{xx}(\omega)= L^{yy}(\omega)$ and $L^{zz}(\omega)$) characterize the edges in the reflection spectra $R(\omega)$ ($R^{xx}(\omega)= R^{yy}(\omega)$ and $R^{zz}(\omega)$). Such as the major peak of are positioned above 10.0 eV (Fig. 4b) is at an energy to the immediate reduction of $R(\omega)$ (Fig. 5c). There is weak anisotropy in the two tensor components of all the optical parameters.

The three components ($R^{xx}(\omega)= R^{yy}(\omega)$ and $R^{zz}(\omega)$) of the reflectivity spectra $R(\omega)$ reveal 60.0 % of reflections at 14.0 eV (Fig. 5c). That clarifies that that the investigated compound can be used as a possible shield for ultraviolet radiation. The reflectivity spectra weak anisotropy among the components. It can be deduced that at low energies there exist a small reflectivity, then an increase occurs in the reflectivity at high energies. Generally the maxima in the reflectivity occurs due to the inter-band transitions.

The important parameter is the refractive index, $N(\omega)=n(\omega)+ik(\omega)$ n and k symbolize for the refractive index and extinction coefficient. Understanding about the refractive index n, this can give much valuable information regarding the optical properties of the substance. The k (extinction coefficient) is also recognized as the damping constant or attenuation coefficient, that illustrates the decrease of the electromagnetic waves (EMW) in the material. The expression about n and k and about the dielectric function $\varepsilon(\omega)$ is expressed as:

$\mathrm{Re}(\varepsilon)=n^2+k^2; \mathrm{Im}(\omega)=2nk$.

The $n(\omega)$ has a direct link with the optical $I(\omega)$ (absorption spectra). The investigated spectra for the $n(\omega)$ (see Fig.) shows the maximum value occurs in the energy range between 5.0 ~ 6.0 eV optical frequency for $n^{xx}(\omega)= n^{yy}(\omega)$ and $n^{zz}(\omega)$. Comparing the $n(\omega)$ spectra shows very close behavior to the $\varepsilon_1(\omega)$ spectra and shows that $n(\omega)$ at low frequencies has the inverse relation with the width of the band gap. The investigated $n(\omega)$ spectra exhibit substantial anisotropy that formed from the anisotropy of the dielectric function. The static refractive indices is close to $n^{xx}(0)= n^{yy}(0)$ and $n^{zz}(0)$ are 2.0 and 1.75. With increasing the energy (i.e. above 7.0 eV), the curve tends to decrease and crosses the unity at around 10.0 eV. When $n < k$, the compounds exhibit metallic possessions, and the photon frequency range is known as the metal reflective region (MRR).

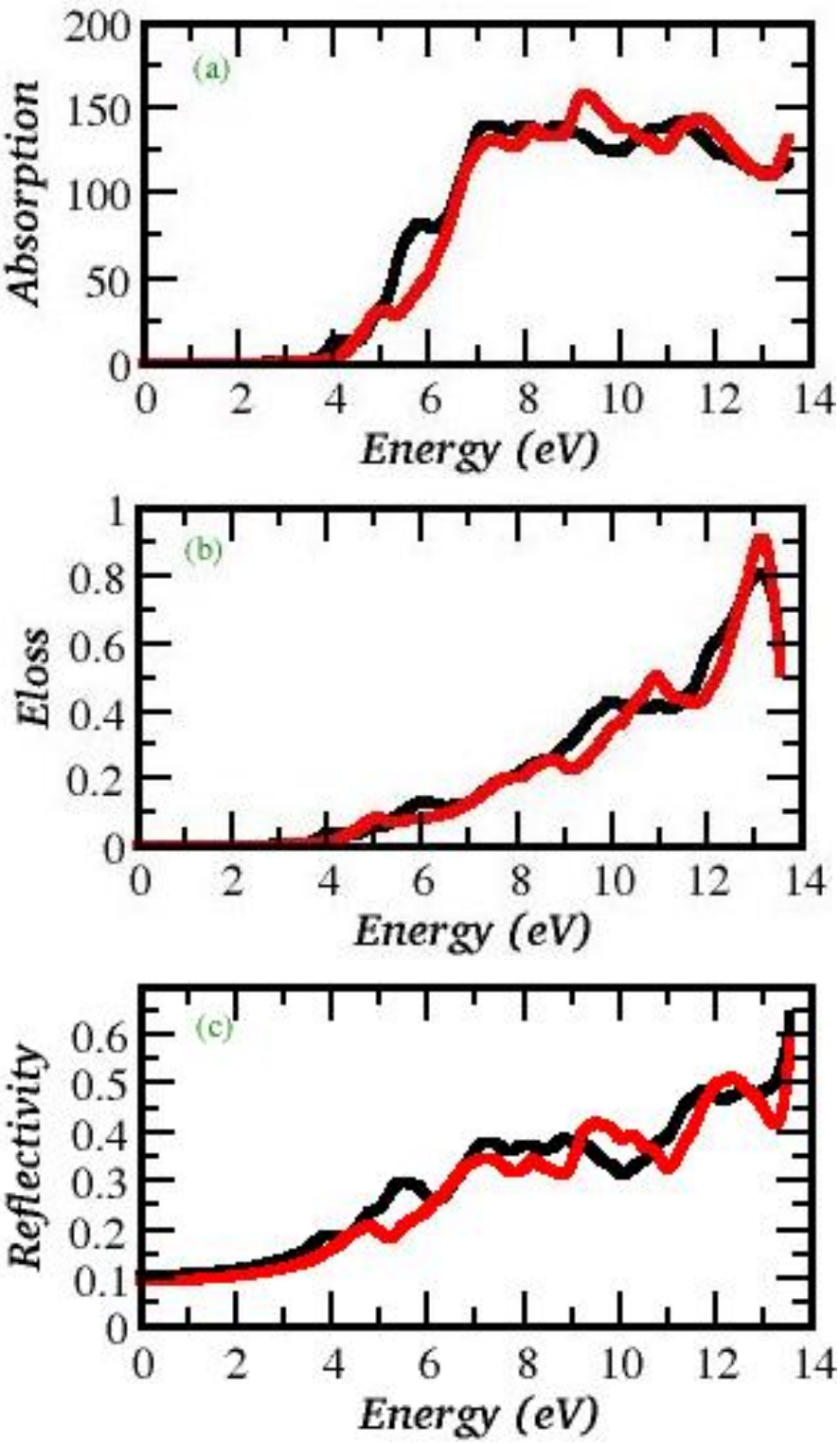
(a)
Absorption
200
150
100
50
0
0 2 4 6 8 10 12 14
Energy (eV)
(b)
Eloss
1
0.8
0.6
0.4
0.2
0
0 2 4 6 8 10 12 14
Energy (eV)
(c)
Reflectivity
0.6
0.5
0.4
0.3
0.2
0.1
0
0 2 4 6 8 10 12 14
Energy (eV)

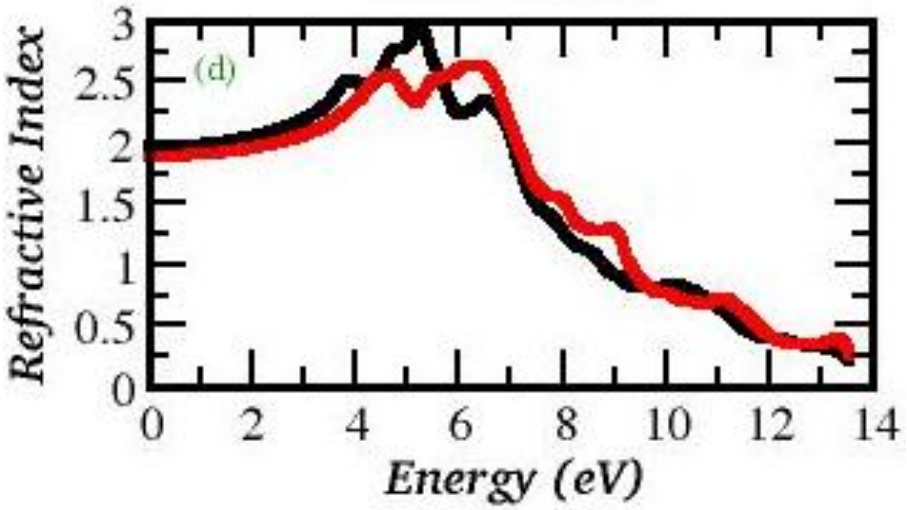

Figure 6. (a) Calculated Absorption $I^{\circ}(\omega)$ spectra of Li_3AlH_6 (b) Calculated energy-loss spectrum $L^{xx}(\omega)$ spectra of Li_3AlH_6 (c) Calculated reflectivity $R^{xx}(\omega)$ of Li_3AlH_6 (d) Calculated refractive index $n^{\circ}(\omega)$ spectra of Li_3AlH_6

3. CONCLUSION

In this research, the first-principles full potential method of density functional theory combined with the generalized gradient approximation method is used to compute the electronic structure and optical properties of lithium metal hydride crystal (Li_3AlH_6) for hydrogen storage. Firstly we performed the optimization. The band structures of crystals exhibit that the investigated material shows indirect band gap of 2.97 eV (N-Γ) thus, the material is electronically semiconducting. The crystal structure and opto-electronic properties of these hydrides are newly presented in this study. The absorption peaks are related to photo transitions energies from maximum valence band to minimum conduction band. It is predictable that these novel results are beneficial in terms of solid state hydrogen storage and serving as a reference data to literature.

ACKNOWLEDGEMENTS
The author (A. Dahshan) gratefully thank the Deanship of Scientific Research at King Khalid University for the financial support through research groups program under grant number (R.G.P.2/113/41).

References

1. T. Ghellab, V. Charifi, H. Baaziz, S. Uğur and G. Uğur, *Phys. Scr.*, 91 (2016) 045804.
2. T. Zhang, H. Miyaoka, T. Ichikawa and Y. Kojima**,** *ACS Appl. Energy Mater.*, 1 (2018) 232.
3. D. Guendouz, H. Charifi, T. Baaziz, N. Ghellab, S. Arikan and G. Uğur, *Can. J. Phys.*, 94 (2016) 865.
4. S. I. Orimo, Y. Nakamori, J.R. Eliseo, A. Zuttel and C.M. Jensen, *Chem. Rev.*, 107 (2007) 4111.
5. G. Sandrock, S .Suda and L. Schlapbach, *Hydrogen in Intermetallic Compounds*, 67 (1992) 197.
6. G. Sandrock and Y.Yurum, *Kluwer Acad. Pub.*, 253 (1994) 2

7. C. Carpetis and W. Peshka, *Int. J. Hydrog. Energy*, 1980, 5, 539.
8. R. Agarwal, K. Noh, J. Schwarz and J. Davini, *R. Carbon*, 25 (1987), 219.
9. A.C. Dillion, K.M Jones, T.A. Bekkedahl, C.H Kiang, C.H. Bethune and D.S. Heben, *Nature*, 386 (1997) 377.
10. C. Park, P.E Anderson, A. Chambers, C.D. Tan, R. Hidago and N.M. Rodriquez, *J. Phys. Chem.,* 103 (1999), 10572.
11. C. Liu, Y. Fan, M. Liu, Y.L. Wei, M.Q. Lu and H.M. Cheng, *M. Science,* 286 (1999), 1127.
12. J. Bellosta, J.R Ares, J. Barale, M. Baricco, C. Buckley and G. Capurso, *Int. J. Hydrog. Energy*, 44 (2019) 7780.
13. S.S .Srinivasan and D.E. Demirocak, *Springer Sci. Rev.,* 225 (2017) 255.
14. H. Smithson, C.A. Marianetti, D. Morgan, A.V. Ven, A. Predith and G. Ceder, *Phys. Rev. .,* 66 (2002) 144107.
15. J.H.N.V. Vucht, F.A. Kuipers and H.C.A.M. Bruning, *Phillips Res. Rep.,* 25,(1970) 133.
16. P.Blaha, K. Schwarz, J. Luitz. WIEN97, A full potential linearized augmented plane wave package for calculating crystal properties, Karlheinz Schwarz. Techn. Universit at Wien, Austria, (1991) ISBN:3-9501031-0-4.
17. J.P. Perdew and A. Zunger, *Phys. Rev. B*, 23 (1981) 5048.
18. J.P. Perdew, K. Burke and M. Ernzerho, *Phys. Rev. Lett*., 77 (1996) 3865.
19. F. Tran and P. Blaha, *Phys. Rev. Lett.,* 102 (2009) 226401.
20. J.A. Wilson and A.D. Yoffe, *Adv. Phys*., 18 (1969) 193.
21. D.R. Penn, *Phys. Rev. B,* 128 (1962) 2093.